

# Energy-Efficient Approximate Full Adders Applying Memristive Serial IMPLY Logic For Image Processing\*

Seyed Erfan Fatemieh<sup>†</sup>, and Mohammad Reza Reshadinezhad<sup>†</sup>

June 11, 2024

## Abstract

Researchers and designers are facing problems with memory and power walls, considering the pervasiveness of Von-Neumann architecture in the design of processors and the problems caused by reducing the dimensions of deep sub-micron transistors. Memristive Approximate Computing (AC) and In-Memory Processing (IMP) can be promising solutions to these problems. We have tried to solve power and memory wall problems by presenting the implementation algorithm of four memristive approximate full adders applying the Material Implication (IMPLY) method. The proposed circuits reduce the number of computational steps by up to 40% compared to State-of-the-art (SOA). The energy consumption of the proposed circuits improves over the previous exact ones by 49%-75% and over the approximate full adders by up to 41%. Multiple error evaluation criteria evaluate the computational accuracy of the proposed approximate full adders in three scenarios in the 8-bit approximate adder structure. The proposed approximate full adders are evaluated in three image processing applications in three scenarios. The results of application-level simulation indicate that the four proposed circuits can be applied in all three scenarios, considering the acceptable image quality metrics of the output images (the Peak Signal to Noise Ratio (PSNR) of the output images is greater than 30 dB).

## Keywords

Approximate Computing, Approximate Full Adder, Memristor, IMPLY logic, Image Processing, In-Memory Processing.

## 1 Introduction

The power wall is a considerable adversity in the computer architects' path [1]. Energy consumption in portable electronic devices becomes a significant challenge with the invalidation of Dennard's scaling, deviation from Moore's law, and the occurrence of problems with the reduction of transistor dimensions, such as increased leakage currents, short channel effects, reduced reliability, and increased manufacturing costs [2–8]. The difference in the speed of memories and processors and Von-Neumann's memory wall bottleneck is another challenge in the design of digital systems [1, 9–11].

Several solutions to overcome the power wall problem have been proposed to date. One of the solutions welcomed by researchers and technology companies like IBM in recent years is AC [2–4, 12–14]. In AC, the accuracy of computations is reduced to an acceptable level. In exchange for this reduction in accuracy, designers can reduce circuit complexity (energy consumption, delay, and area). AC cannot be applied in all aspects of computations because the accuracy of computations must be 100% in some processing applications. Error-resistant applications such as image processing, pattern recognition, machine learning, digital signal processing, and data mining are among the applications in which AC can be applied [2, 4, 14–17]. For example, in image processing, reasons such as

---

\*Preprint Submitted to arXiv

<sup>†</sup>S. E. Fatemieh and M. R. Reshadinezhad are with the Department of Computer Architecture, Faculty of Computer Engineering, University of Isfahan, Isfahan 8174673441, Iran (email: erfanfatemieh@eng.ui.ac.ir; m.reshadinezhad@eng.ui.ac.ir) (*Corresponding author: Mohammad Reza Reshadinezhad*).

a small error in the output pixels due to data noise or approximately performing computations affect the quality of the images [2, 15, 17]. However, humans' limited visual perception accepts the results [2–4, 17, 18].

The idea of applying processing units next to the main memory (due to the impossibility of data processing by the Dynamic Random Access Memory (DRAM) cell) has been applied by researchers for decades to overcome the memory wall. One of the proposed methods to overcome the memory wall is IMP. With the advancement of technology and the introduction of memristors, it is possible to apply IMP more than ever before. A memristor is an electrical element that maintains its previous resistance value when voltage and current are not applied to it and is contemplated as a memory cell [19–21]. As a memory element and in stateful logic, the High Resistance State (HRS) of a memristor is considered as logic '0', and its Low Resistance State (LRS) is considered as logic '1' [3, 10, 14, 22]. Different memory technologies have been contemplated for IMP. However, Resistive RAM (ReRAM) is a popular option among emerging memory technologies for IMP due to its small size, suitable writing speed, low energy consumption, and acceptable endurance [11, 19, 23, 24]. ReRAMs fit well in crossbar array structure and harmonize entirely with current manufacturing technology [3, 10, 19]. There are several methods for designing computing structures applying memristors. Among the most important of these methods, Memristor Aided loGIC (MAGIC), fast and energy-efficient logic in memory (FELIX), and IMPLY can be mentioned [11, 19, 21, 24–26].

Arithmetic circuits are one of the most critical units of each processor. Adders are the central pillar of computing circuits. For example, many instructions in digital signal processing (DSP) processors require adder and multiplier units [3, 27]. So far, many approximate adders have been introduced in different technologies for error-resilient applications that fit today's typical architecture [3, 4, 13–16, 18, 28–30]. In [3, 14, 31, 32], approximate memristor-based full adders are proposed by applying the IMPLY logic for IMP. In this article, AC and IMP by memristors and IMPLY method are applied side by side, and four approximate full adders are proposed for error-resilient applications. Contributions made in this article include:

1. Proposing a compact approximate full adder with Exact  $C_{out}$  and Inexact  $Sum$  (ECIS) to prevent the propagation of the wrong carry digit from the Least Significant Bits (LSBs) to the Most Significant Bits (MSBs) and improve energy consumption and the number of computational steps compared to the exact full adders,
2. Presentation of three compact approximate full adders with Inexact  $C_{out}$  and Inexact  $Sum$  (ICIS1-3) to reduce the number of computational steps and energy consumption compared to the previous designs,
3. Evaluating the accuracy of computations by multiple error evaluation criteria,
4. Evaluation of the proposed approximate full adders in three image processing applications to ensure the accuracy of computations in error-resilient applications in three different scenarios,
5. Presenting a Figure of Merit ( $FOM$ ) to evaluate the proposed circuits by circuit evaluation criteria and accuracy metrics simultaneously.

The rest of the article is arranged in 4 sections. In the second section, the backgrounds of this research are explained, and SOA is briefly introduced and reviewed. In the third section, the implementation algorithms of ECIS and ICIS1-3 full adders are introduced, and their design details are explained. The fourth section evaluates and compares the proposed circuits and SOA by circuit evaluation criteria, error analysis metrics, and image quality metrics. In subsection 4.4, the proposed approximate full adders are also evaluated by a  $FOM$  to have a comprehensive view of the reduction of circuit complexity and the reduction of accuracy in the computations of the proposed circuits. Section 5 contains the conclusion of the article.

## 2 Backgrounds

### 2.1 Approximate computing

Reducing the accuracy of computations by applying AC in data-intensive error-resilient applications, such as image processing, can unravel the hardware complexity of these applications. AC has been applied to design circuits from memory to arithmetic circuits, such as adders and multipliers [3–5, 13–18, 27–30]. Designers should focus on the compromise between reducing the accuracy of computations and hardware complexity (reducing

energy consumption and increasing efficiency) in applications where AC is applied. The reasons for applying AC can be limited visual perception of humans, lack of only one acceptable answer, resistance to input noise, and error coverage and attenuation [2, 17]. Among the essential error-resilient applications are image processing, deep learning, robotics, data mining, and pattern recognition [2, 15–17].

To design approximate arithmetic circuits, circuit evaluation criteria such as energy consumption, performance, and area dissipation should be evaluated to ensure the improvement of circuit evaluation criteria. The evaluation of the accuracy of computations is critical from two different aspects. The first aspect is the examination of standard error evaluation criteria such as Error Rate (ER), Error Distance (ED), Mean ED (MED), and Normalized MED [15]. By examining these criteria, one can get a general view of the accuracy of computations by applying the designed approximate circuit in different computing structures. The method of calculating these error evaluation criteria is described in [3, 4, 15, 16]. In general, the smaller the error evaluation criteria, the higher the accuracy of the computation. The second aspect is to pay attention to the application in which the proposed circuits are applied. The specific output evaluation criteria of the desired application should also evaluate the designed approximate arithmetic circuits. In the application of image processing, in which the proposed approximate circuits are applied in this paper, image quality evaluation criteria such as PSNR, Structural Similarity Index (SSIM), and Mean SSIM (MSSIM) should be assessed to ensure the proper performance of the approximate arithmetic circuits [3, 4, 12–18, 33]. The criteria for evaluating the quality of images and their importance were studied in [12, 34]. The greater the image quality evaluation criteria, the better the quality of the output images. The output image is acceptable and of good quality when the image created by the approximate circuit has a PSNR greater than 30 dB [33].

## 2.2 Memristors

Emerging non-volatile memory technologies have attracted the attention of researchers in recent years, considering the importance of memory cells in all processing structures and the limitations caused by reducing the dimensions of transistors, especially in flash memories [19]. A memristor is an electrical element introduced by Leon Chua in 1971 [19]. Memristors can keep their previous state, and this feature makes them a suitable alternative to today’s standard memory technologies. ReRAM has become a prevalent choice for replacing conventional memory technologies among researchers due to its unique features compared to other emerging memory technologies such as Ferroelectric RAM (FeRAM), Phase Change Memory (PCM), and Magnetic RAM (MRAM) [19, 35].

So far, several logical design methods have been presented for circuit design applying memristors [11, 19, 21, 24, 26]. Each of these methods has its characteristics. Statefulness is one of the essential features to consider for implementing memristor-based circuits [3, 19, 25, 36]. In the implementation of a circuit, if the input, intermediate nodes, and output states of a circuit are represented by resistance, the design method of that circuit is stateful [19]. In order to be able to perform IMP applying memristors, stateful design methods should be applied [19, 25]. One of the stateful and flexible memristor-based circuit design methods introduced by Hewlett-Packard (HP) is IMPLY [3, 14, 19]. The structure of the IMPLY function is shown in Figure 1, and its truth table is written in Table 1. In IMPLY logic, the inputs are set to HRS and LRS in memristors  $p$  and  $q$ , and after performing the IMPLY operation, the result is written in memristor  $q$  [21]. The following conditions must be met to perform IMPLY correctly [3, 10, 14, 21, 22]:

1.  $V_{COND} < V_c < V_{SET}$ ,  $V_c$  is the threshold voltage of a memristor.
2.  $R_{ON} \ll R_G \ll R_{OFF}$

All the logical functions (e.g., Nand, Nor, and Xor) can be implemented by applying IMPLY and FALSE (zero) functions in different numbers of computational steps. Algorithms for implementing different logic functions applying the IMPLY method are analyzed in [20].

## 2.3 Exact and approximate memristor-based adders

### 2.3.1 IMPLY-based adders’ architectures

Four serial, parallel, semi-serial, and semi-parallel architectures were introduced to implement the algorithms of arithmetic structures (e.g., n-bit adders) applying IMPLY method [10, 11, 20–22].

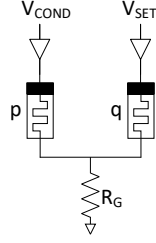


Figure 1: Circuit design of a memristive IMPLY logic gate [10].

Table 1: The truth table of an IMPLY logic gate.

p	q	p IMPLY q $\equiv$ p $\rightarrow$ q
0	0	1
0	1	1
1	0	0
1	1	1

In serial architecture, memristors are placed next to each other in a row/column and connected to the ground by a resistor. Only a FALSE or an IMPLY operation can be executed in each computational step. The serial architecture of an n-bit adder is shown in Figure 2. Serial architecture has the simplest structure compared to other architectures. It can be well implemented in the structure of crossbar arrays [20]. Due to the simplicity of the serial architecture and the impossibility of executing two instructions simultaneously, the number of computational steps in this method is more than in the other architectures.

In parallel architecture, memristors are placed in rows (or columns) parallel to each other. Each row/column is connected to a resistor of that row/column by a switch and to other rows/columns by another switch (see Figure 3). If there is no dependency between the memristors of consecutive steps in an implementation algorithm, the instructions applying this architecture can be calculated simultaneously [37]. However, suppose there is a dependency between the memristors of consecutive instructions. In that case, it is impossible to execute several instructions in parallel, e.g., to calculate the  $C_{out}$  of a full adder proposed in [37]. Parallel architecture has the maximum hardware complexity compared to other architectures, but the number of computational steps of different algorithms in this architecture is less than in the other architectures [10, 22].

In [10, 22], semi-parallel and semi-serial architectures for implementing n-bit adders are introduced. In both architectures, the input memristors (input numbers  $A$  and  $B$ ) are placed in two separate rows. In the semi-parallel architecture (see Figure 4), there is a work memristor in each line ( $w_1$  and  $w_2$ ), and the  $C_{in}$  memristor is placed in the second row [22]. Each row is connected to a resistor by a switch, and another switch connects two rows [22]. In the semi-serial method (see Figure 5), each row is directly connected to a resistor [10]. Each of the work memristors ( $c$  and  $w_1-w_4$ ), along with the  $C_{in}$  memristor, can be connected to the input memristors of each of the upper or lower rows by two different switches and perform the desired operation in this architecture [10].

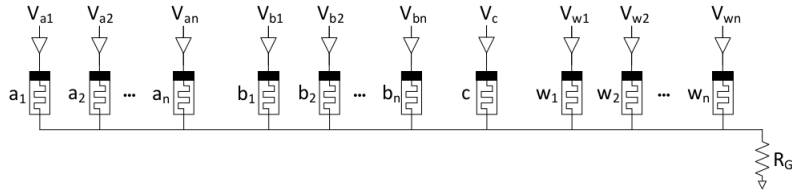


Figure 2: The serial architecture of an IMPLY-based n-bit adder [10].

### 2.3.2 IMPLY-based exact full adders

The importance of the full adder cell in all kinds of computing structures suitable for Von-Neumann architecture and IMP is obvious. For this reason, researchers have introduced multiple IMPLY-based full adders in recent years [10, 20–22, 37]. These full adders are designed based on all four architectures introduced in section 2.3.1. The

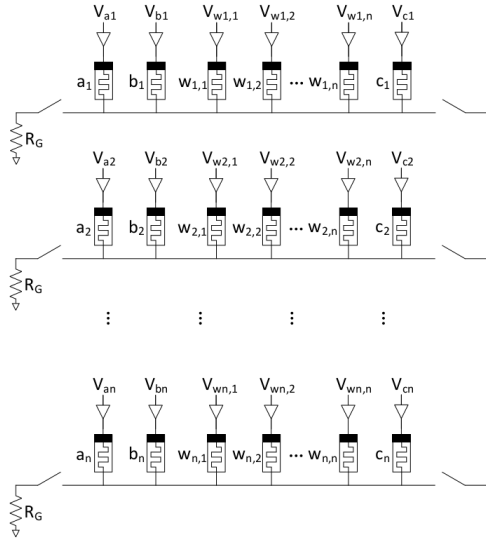


Figure 3: The parallel architecture of an IMPLY-based  $n$ -bit adder [10].

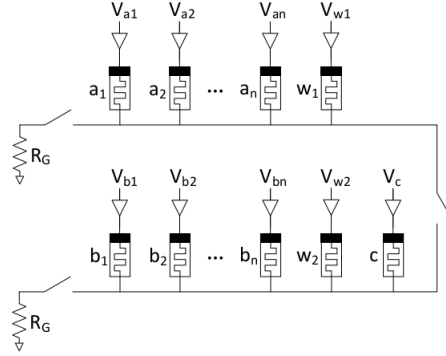


Figure 4: The semi-parallel architecture of an IMPLY-based  $n$ -bit adder [10].

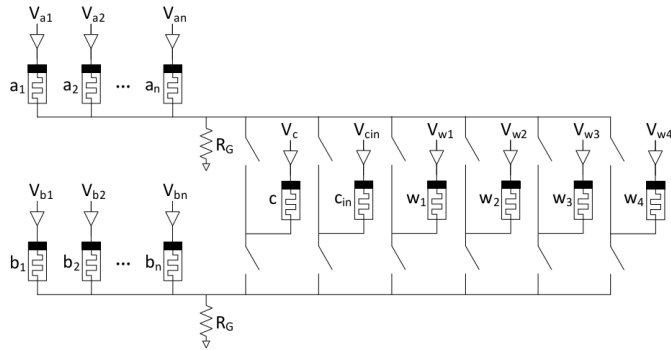


Figure 5: The semi-serial architecture of an IMPLY-based  $n$ -bit adder [10].

number of required memristors, computational steps, and CMOS switches are among the most critical criteria differentiating these circuits. In Table 2, some of the most prominent IMPLY-based exact full adders introduced are compared with each other along with their features in the architecture applied [10, 20–22, 37].

Full adders introduced in serial architecture have less structural complexity than other full adders. However, circuits designed based on this method need more computational steps than other methods to function correctly [10].

Table 2: Comparison between IMPLY-based exact full adders.

Architecture	No. of memristors	No. of steps	No. of switches
Serial [20]	5	22	0
Serial [37]	5	23	0
Parallel [21]	9	23	2
Parallel [37]	5	21	1
Semi-parallel [22]	5	17	3
Semi-serial [10]	8	12	12

### 2.3.3 IMPLY-based approximate full adders

To the best of our knowledge, the first approximate full adder based on the IMPLY logic was introduced in [14]. This full adder computes  $Sum$  and  $C_{out}$  outputs in 8 computational steps with only five memristors [14]. The main problem of this approximate full adder is that the outputs are written in work memristors. As the number of approximate full adders increases in the n-bit approximate adder structure, the number of required memristors increases. The authors in [3] solved the problem of their previously proposed approximate full adder introduced in [14] by modifying its implementation algorithm. In [3], four Serial IMPLY-based approximate full adders (SIAFA1-4) are introduced. SIAFA1-4 require four/five memristors (three input memristors and one/two work memristors) to implement and compute the outputs in 8, 10, 8, and 8 computational steps, respectively [3]. Serial Approximate Full Adder using NAND gates (SAFAN) is another IMPLY-based approximate full adder that was proposed recently [31]. This approximate full adder is designed and implemented in serial architecture like the ones proposed in [3, 14]. The implementation algorithm of SAFAN computes the outputs in seven computational steps by applying four memristors (three input memristors and one work memristor) [31]. Seiler et al. proposed an approximate full adder cell (semi-serial AFA) compatible with the semi-serial architecture [32]. The  $Sum$  and  $C_{out}$  outputs of this full adder are computed in six computational steps with five memristors [32]. Error evaluation metrics of ED, MED, and NMED were calculated for the approximate full adders proposed in [3, 31, 32]. The circuit and error evaluation criteria of SIAFA1-4, SAFAN, and semi-serial AFA are summarized and written in Table 3. SAFAN, SIAFA1-4, and semi-serial AFA was evaluated in image processing applications, too [3, 31, 32].

Table 3: The circuit and error evaluation criteria of SIAFA1-4 [3], SAFAN [31], and semi-serial AFA [32].

Approximate full adder	No. of steps	No. of memristors	No. of switches	ED	MED	NMED
SIAFA1 [3]	8	4	0	3	0.375	0.125
SIAFA2 [3]	10	5	0	4	0.5	0.166
SIAFA3 [3]	8	4	0	3	0.375	0.125
SIAFA4 [3]	8	4	0	3	0.375	0.125
SAFAN [31]	7	4	0	3	0.375	0.125
Semi-serial AFA [32]	6	5	6	3	0.375	0.125

### 2.3.4 An overview of non-stateful memristor-based approximate full adders

One of the non-stateful memristor-based arithmetic circuit design methods is the Memristor Ratioed Logic (MRL) [11, 19]. This method creates AND and OR gates by connecting two memristors in series according to their polarities [11, 19]. The logical states of the inputs and outputs of the MRL-based circuits are determined by voltage levels, like Complementary Metal Oxide Semiconductor (CMOS) circuits [11, 19]. There is a voltage drop problem in the MRL method's output signals, so some intermediate nodes need buffers to restore the signal level [19]. Using these buffers and signal transmission between memristors, vias, and transistors is associated with energy loss and affects the delay [3].

Different exact and approximate full adders were introduced by applying this method [11, 19, 38–40]. An MRL-based exact full adder was introduced in [38, 39]. This full adder consists of 33 memristors and some inverters [38, 39]. Two MRL-based approximate full adders were proposed based on redefining approximate logic from the exact logic method in [38, 39]. These approximate full adders are implemented with 10 and 14 memristors

and by applying some inverters to restore signal levels [38, 39]. These approximate full adders were evaluated in the application of image addition, and the output results were assessed with PSNR [3, 38, 39].

## 2.4 Approximate full adders in CMOS and emerging technologies

In more than a decade and due to the importance of the full adder cell, several approximate full adders applying MOSFET transistors were introduced as today’s standard manufacturing technology and evaluated in various error-resilient applications [4, 15, 16, 18]. Several approximate full adders were introduced in emerging technologies such as Carbon Nano Tube (CNT) FET and Quantum Cellular Automata (QCA), and their efficiency was evaluated in error-tolerant applications [28–30]. In most cases, these approximate circuits are designed based on redesigning the approximate logic from the exact logic method by rearranging the circuits and their input and altering the exact full adder’s truth table to the approximate one [4, 18, 28–30].

## 3 Proposed IMPLY-based approximate full adders

In this section, the proposed circuits and their design method are described. In subsection 3.1, three approximate full adders are introduced to reduce the hardware complexity along with an acceptable decrease in computation accuracy. In subsection 3.2, the primary purpose of proposing an approximate full adder is to avoid inexact carry propagation from LSBs to MSBs in an n-bit approximate adder structure.

### 3.1 Inexact Carry, Inexact Sum IMPLY-based approximate full adders (ICIS)

Three ICIS full adders (ICIS1-3) are designed in three steps and based on redesigning approximate logic from exact logic by changing the exact full adder’s truth table. It is necessary to determine the conditions of acceptability of approximate full adders’ accuracy before explaining the design steps of the proposed circuits. The maximum value of  $ER_{Sum}$  and  $ER_{C_{out}}$  should be  $\frac{3}{8}$  and  $\frac{1}{8}$  to have acceptable output results based on the error analysis metrics of SOA [3, 4, 14–16, 18, 29] in error-tolerant applications, e.g., image processing. According to these ERs, the maximum acceptable value of ED for the design of the proposed approximate full adders is also considered 3. Determining these conditions for designing ICIS1-3 is done because the reduction of computation’s accuracy should be limited. In addition to the error evaluation criteria, the computational steps should be significantly reduced compared to the exact full adders. The number of computational steps affects energy consumption directly.

The design steps of ICIS1-3, according to the mentioned design constraints, are:

**STEP 1:** First, the truth table of the exact full adder is assessed (see Table 4). Then, according to the design constraints mentioned above, the  $C_{out}$  of the exact full adder is inverted only in the first state ( $A_{in}B_{in}C_{in} = \text{“000”}$ ), and  $ER_{C_{out}}$  is  $\frac{1}{8}$ . In IMPLY logic, it is possible to invert an output in only two computational steps. In the first step, a memristor resets; in the second cycle, IMPLY function performs between the output memristor and the one reset in the last cycle. The  $Sum$  output of these approximate full adders is assumed to be  $\overline{C_{out}}$  to reduce the hardware complexity and the number of computational steps. This process is repeated for states 2 ( $A_{in}B_{in}C_{in} = \text{“001”}$ ) to state 8 ( $A_{in}B_{in}C_{in} = \text{“111”}$ ) of the exact full adder. Eight approximate full adders’ truth tables are designed by applying this method. We call these eight Approximate Full Adders AFA1-8. These eight approximate full adders’ truth tables can be seen next to the exact full adder’s truth table in Table 4. The truth tables of approximate full adders display exact outputs with  $\checkmark$  and inexact ones with a  $\times$ . ED of each AFA is specified in Table 4.  $ER_{C_{out}}$  of these eight approximate full adders is  $\frac{1}{8}$ . The  $ER_{Sum}$  of AFA2-7 is  $\frac{3}{8}$ , and the  $ER_{Sum}$  of AFA1 and AFA8 equals  $\frac{1}{8}$ . It should be noted that the ED of all these approximate full adders equals 3. Among the AFA1-8 (see Table 4), the truth tables of AFA4, AFA6, and AFA7 are similar to those of SIAFA3, SIAFA1, and SIAFA4 introduced and implemented in our previous research [3]. So, AFA1-3, 5, and 8 are considered implementation candidates according to the error analysis metrics, and the truth table of these approximate full adders is not the same as the truth tables of SIAFA1, SIAFA3, and SIAFA4 [3].

This time the truth table of eight approximate full adders is generated by inverting one bit of the exact full adder’s  $Sum$  output from state  $A_{in}B_{in}C_{in} = \text{“000”}$  to state  $A_{in}B_{in}C_{in} = \text{“111”}$  similar to what was done for exact  $C_{out}$ . This time,  $C_{out}$  equals  $\overline{Sum}$ , and  $C_{out}$  can be calculated with only two computational steps. The truth tables of Approximate Full Adders 9-16, AFA9-16, are tabulated in Table 5. According to this design method, the  $ER_{Sum}$  of these approximate full adders equals  $\frac{1}{8}$ . As in Table 4, the ED of AFA9-16 is written in the last row of

Table 4: The truth tables of exact full adder and AFA1-8.

$A_{in}$	$B_{in}$	$C_{in}$	Exact $Sum$	Exact $C_{out}$	AFA1 $Sum$	AFA1 $C_{out}$	AFA2 $Sum$	AFA2 $C_{out}$	AFA3 $Sum$	AFA3 $C_{out}$	AFA4 $Sum$	AFA4 $C_{out}$	AFA5 $Sum$	AFA5 $C_{out}$	AFA6 $Sum$	AFA6 $C_{out}$	AFA7 $Sum$	AFA7 $C_{out}$	AFA8 $Sum$	AFA8 $C_{out}$
0	0	0	0	0	0✓	1✗	1✗	0✓	1✗	0✓	1✗	0✓	1✗	0✓	1✗	0✓	1✗	0✓	1✗	0✓
0	0	1	1	0	1✓	0✓	0✗	1✗	1✓	0✓	1✓	0✓	1✓	0✓	1✓	0✓	1✓	0✓	1✓	0✓
0	1	0	1	0	1✓	0✓	1✓	0✓	0✗	1✗	1✓	0✓	1✓	0✓	1✓	0✓	1✓	0✓	1✓	0✓
0	1	1	0	1	0✓	1✓	0✓	1✓	0✓	1✓	1✗	0✗	0✓	1✓	0✓	1✓	0✓	1✓	0✓	1✓
1	0	0	1	0	1✓	0✓	1✓	0✓	1✓	0✓	1✓	0✓	0✗	1✗	1✓	0✓	1✓	0✓	1✓	0✓
1	0	1	0	1	0✓	1✓	0✓	1✓	0✓	1✓	0✓	1✓	0✓	1✓	1✗	0✗	0✓	1✓	0✓	1✓
1	1	0	0	1	0✓	1✓	0✓	1✓	0✓	1✓	0✓	1✓	0✓	1✓	0✓	1✓	1✗	0✗	0✓	1✓
1	1	1	1	1	0✗	1✓	0✗	1✓	0✗	1✓	0✗	1✓	0✗	1✓	0✗	1✓	0✗	1✓	0✗	1✓
					ED=3		ED=3		ED=3		ED=3		ED=3		ED=3		ED=3		ED=3	

Table 5: The truth tables of AFA9-16.

$A_{in}$	$B_{in}$	$C_{in}$	AFA9 $Sum$	AFA9 $C_{out}$	AFA10 $Sum$	AFA10 $C_{out}$	AFA11 $Sum$	AFA11 $C_{out}$	AFA12 $Sum$	AFA12 $C_{out}$	AFA13 $Sum$	AFA13 $C_{out}$	AFA14 $Sum$	AFA14 $C_{out}$	AFA15 $Sum$	AFA15 $C_{out}$	AFA16 $Sum$	AFA16 $C_{out}$
0	0	0	1✗	0✓	0✓	1✗	0✓	1✗	0✓	1✗	0✓	1✗	0✓	1✗	0✓	1✗	0✓	1✗
0	0	1	1✓	0✓	0✗	1✗	1✓	0✓	1✓	0✓	1✓	0✓	1✓	0✓	1✓	0✓	1✓	0✓
0	1	0	1✓	0✓	1✓	0✓	0✗	1✗	1✓	0✓	1✓	0✓	1✓	0✓	1✓	0✓	1✓	0✓
0	1	1	0✓	1✓	0✓	1✓	0✓	1✓	1✗	0✗	0✓	1✓	0✓	1✓	0✓	1✓	0✓	1✓
1	0	0	1✓	0✓	1✓	0✓	1✓	0✓	1✓	0✓	0✗	1✗	1✓	0✓	1✓	0✓	1✓	0✓
1	0	1	0✓	1✓	0✓	1✓	0✓	1✓	0✓	1✓	0✓	1✓	1✗	0✗	0✓	1✓	0✓	1✓
1	1	0	0✓	1✓	0✓	1✓	0✓	1✓	0✓	1✓	0✓	1✓	0✓	1✓	1✗	0✗	0✓	1✓
1	1	1	1✓	0✗	1✓	0✗	1✓	0✗	1✓	0✗	1✓	0✗	1✓	0✗	1✓	0✗	0✗	1✓
			ED=3		ED=5		ED=5		ED=5		ED=5		ED=5		ED=5		ED=3	

Table 5. AFA9 and AFA16 have acceptable error analysis metrics (See Table 5) based on the conditions specified about the ER and ED of approximate full adders. According to the truth tables of these two circuits, it can be concluded that AFA9 and AFA16 are logically equivalent to AFA1 and AFA8.

Therefore, the output of this step of designing ICIS full adders consists of the truth tables of AFA1-3, AFA5, and AFA8.

**STEP 2:** After determining the truth table of the acceptable circuits from STEP 1, the boolean logic function of the outputs of each circuit must be determined. Based on these functions, an algorithm can be provided for implementing these circuits with IMPLY logic by applying the IMPLY and FALSE functions to memristors. Karnaugh map is one of the methods that can be applied to simplify the boolean output functions of combinational circuits. In this step, the Karnaugh map is applied to simplify and design the output functions of each approximate full adder.

AFA1-3, AFA5 and AFA8 are selected approximate circuits from the previous step. Each of these approximate full adders has two approximate outputs, and for each of the outputs, boolean functions are specified by applying the Karnaugh map. Logic functions of the outputs of AFA1-3, AFA5, and AFA8 are written in (1)-(10), respectively. The output of this step of designing the ICIS full adders is the boolean logic functions of (1)-(10).

$$Sum_{AFA1} = \overline{A_{in}} \cdot (B_{in} \oplus C_{in}) + \overline{C_{in}} \cdot (A_{in} \oplus B_{in}) \quad (1)$$

$$C_{out_{AFA1}} = \overline{Sum_{AFA1}} \quad (2)$$

$$Sum_{AFA2} = \overline{C_{in}} \cdot (\overline{B_{in} \cdot A_{in}}) \quad (3)$$

$$C_{out_{AFA2}} = \overline{Sum_{AFA2}} \quad (4)$$

$$Sum_{AFA3} = \overline{B_{in}} \cdot (\overline{A_{in} \cdot C_{in}}) \quad (5)$$

$$C_{out_{AFA3}} = \overline{Sum_{AFA3}} \quad (6)$$

$$Sum_{AFA5} = \overline{A_{in}} \cdot (\overline{B_{in} \cdot C_{in}}) \quad (7)$$

$$C_{out_{AFA5}} = \overline{Sum_{AFA5}} \quad (8)$$



$$Sum_{AFA8} = \overline{A_{in}} \cdot (\overline{B_{in}} \cdot \overline{C_{in}}) + \overline{B_{in}} \cdot \overline{C_{in}} + A_{in} \cdot B_{in} \cdot C_{in} \quad (9)$$

$$C_{out_{AFA8}} = \overline{Sum_{AFA8}}. \quad (10)$$

**STEP 3:** The logic functions in (1)-(10) are designed based on boolean logic gates. Applying these logic gates in the design of IMPLY-based circuits is impossible. (1)-(10) should be rewritten so that it is possible to implement them by applying IMPLY and FALSE functions. Implementing all boolean logic functions applying IMPLY and FALSE functions is possible. The implementation of binary logic gates required by (1)-(10) can be investigated and studied in [20]. (1)-(10) are rewritten, applying IMPLY and FALSE functions in (11)-(20).

$$Sum_{AFA1} = [B_{in} \rightarrow (\overline{C_{in}} \rightarrow A_{in})] \rightarrow [(((A_{in} \rightarrow C_{in}) \rightarrow (\overline{A_{in}} \rightarrow \overline{C_{in}})) \rightarrow B_{in}) \rightarrow 0] \quad (11)$$

$$C_{out_{AFA1}} = Sum_{AFA1} \rightarrow 0 \quad (12)$$

$$C_{out_{AFA2}} = (B_{in} \rightarrow (A_{in} \rightarrow 0)) \rightarrow C_{in} \quad (13)$$

$$Sum_{AFA2} = C_{out_{AFA2}} \rightarrow 0 \quad (14)$$

$$C_{out_{AFA3}} = (C_{in} \rightarrow (A_{in} \rightarrow 0)) \rightarrow B_{in} \quad (15)$$

$$Sum_{AFA3} = C_{out_{AFA3}} \rightarrow 0 \quad (16)$$

$$C_{out_{AFA5}} = (C_{in} \rightarrow (B_{in} \rightarrow 0)) \rightarrow A_{in} \quad (17)$$

$$Sum_{AFA5} = C_{out_{AFA5}} \rightarrow 0 \quad (18)$$

$$[\overline{B_{in}} \rightarrow C_{in}] \rightarrow [(((B_{in} \rightarrow \overline{C_{in}}) \rightarrow A_{in}) \rightarrow (\overline{B_{in}} \rightarrow (C_{in} \rightarrow \overline{A_{in}})))] \quad (19)$$

$$C_{out_{AFA8}} = Sum_{AFA8} \rightarrow 0 \quad (20)$$

Now, (11)-(20) should be implemented serially by applying a few memristors, three input memristors ( $A_{in}$ ,  $B_{in}$ , and  $C_{in}$ ), and a maximum of two work memristors ( $S_1$  and  $S_2$ ). The serial implementation algorithm of AFA2, AFA3, and AFA5 are written in Tables 6-8, respectively. These three approximate full adders can be implemented in 6 computational steps according to the presented algorithms and by applying four memristors, including three input memristors and a work memristor.

Table 6: AFA2's IMPLY-based implementation algorithm (ICIS1).

Step	Operation	Equivalent logic
1	$S_1 = 0$	$FALSE(S_1)$
2	$A_{in} \rightarrow S_1 = S'_1$	$NOT(A_{in})$
3	$B_{in} \rightarrow S'_1 = S''_1$	$B_{in} \rightarrow NOT(A_{in})$
4	$S''_1 \rightarrow C_{in} = C'_{in}$	$C_{out} = (B_{in} \rightarrow (A_{in} \rightarrow 0)) \rightarrow C_{in}$
5	$A_{in} = 0$	$FALSE(A_{in})$
6	$C'_{in} \rightarrow A_{in} = A'_{in}$	$Sum = \overline{C_{out}}$

The implementation algorithm of AFA1 and AFA8 is written serially by applying IMPLY and FALSE functions according to the output functions of these two approximate full adders, (11), (12), (19), and (20). These approximate full adders are removed from the set of ICIS full adders candidates. The main reason for this decision is that according to the complexity of these two circuits and their implementation algorithms, at least five memristors

Table 7: AFA3's IMPLY-based implementation algorithm (ICIS2).

Step	Operation	Equivalent logic
1	$S_1 = 0$	$FALSE(S_1)$
2	$A_{in} \rightarrow S_1 = S'_1$	$NOT(A_{in})$
3	$C_{in} \rightarrow S'_1 = S''_1$	$C_{in} \rightarrow NOT(A_{in})$
4	$S''_1 \rightarrow B_{in} = B'_{in}$	$C_{out} = (C_{in} \rightarrow (A_{in} \rightarrow 0)) \rightarrow B_{in}$
5	$A_{in} = 0$	$FALSE(A_{in})$
6	$B'_{in} \rightarrow A_{in} = A'_{in}$	$Sum = \overline{C_{out}}$

Table 8: AFA5's IMPLY-based implementation algorithm (ICIS3).

Step	Operation	Equivalent logic
1	$S_1 = 0$	$FALSE(S_1)$
2	$B_{in} \rightarrow S_1 = S'_1$	$NOT(B_{in})$
3	$C_{in} \rightarrow S'_1 = S''_1$	$C_{in} \rightarrow NOT(B_{in})$
4	$S''_1 \rightarrow A_{in} = A'_{in}$	$C_{out} = (C_{in} \rightarrow (B_{in} \rightarrow 0)) \rightarrow A_{in}$
5	$B_{in} = 0$	$FALSE(B_{in})$
6	$A'_{in} \rightarrow B_{in} = B'_{in}$	$Sum = \overline{C_{out}}$

are needed (three input memristors and at least two work memristors) to implement them in 17 computational steps serially. Comparing the computational steps required by these two circuits and their ED with AFA2, AFA3, and AFA5, it can be concluded that the accuracy of computations applying these two circuits will not increase significantly. In contrast, the number of computational steps increases by 65% compared to AFA2, AFA3, and AFA5. So, there would be no justification for presenting these circuits as ICIS approximate full adders.

AFA2, AFA3, and AFA5 are called ICIS1, ICIS2, and ICIS3, respectively, in the rest of the article and Tables 6-8.

### 3.2 Exact Carry, Inexact Sum IMPLY-based approximate full adder (ECIS)

The primary purpose of designing ECIS is to improve its error evaluation criteria compared to ICIS1-3. Applying this full adder avoids error propagation from the LSBs to MSBs in n-bit approximate adders. The ECIS full adder is designed in three steps, like ICIS1-3. These three steps are:

**STEP 1:** Designing an approximate full adder in which its  $C_{out}$  is computed accurately is a solution to prevent error propagation from the LSBs. In ECIS, the  $C_{out}$  is exact, and the  $Sum$  is considered  $\overline{C_{out}}$ . The truth table of ECIS can be seen in Table 9. According to Table 9, this approximate full adder's  $ER_{Sum}$  is  $\frac{2}{8}$ , and  $C_{out}$  is calculated precisely ( $ER_{C_{out}}$  is 0). The ED of ECIS is 2. As in Tables 4 and 5, the exact states are marked with a ✓, and the inexact states are labeled with a ✗. By examining the error evaluation criteria, it can be concluded that the accuracy of ECIS computations will be higher than ICIS1-3.

Table 9: The truth tables of exact full adder and ECIS.

$A_{in}$	$B_{in}$	$C_{in}$	Exact $Sum$	Exact $C_{out}$	ECIS $Sum$	ECIS $C_{out}$
0	0	0	0	0	1 ✗	0 ✓
0	0	1	1	0	1 ✓	0 ✓
0	1	0	1	0	1 ✓	0 ✓
0	1	1	0	1	0 ✓	1 ✓
1	0	0	1	0	1 ✓	0 ✓
1	0	1	0	1	0 ✓	1 ✓
1	1	0	0	1	0 ✓	1 ✓
1	1	1	1	1	0 ✗	1 ✓
					ED=2	

**STEP 2:** In this step, the logic functions of the outputs of ECIS are written in (21) and (22) according to Table 9 and by applying the Karnaugh map. (21) and (22), as outputs of this step, should be implemented serially by

applying IMPLY and FALSE functions.

$$Sum_{ECIS} = (\overline{B_{in}} \cdot (\overline{A_{in}} \cdot C_{in})) + (\overline{A_{in}} + C_{in}) \quad (21)$$

$$C_{out_{ECIS}} = \overline{Sum_{ECIS}} \quad (22)$$

**STEP 3:** A serial algorithm and five memristors (three input memristors and a maximum of two work memristors) are needed to implement an IMPLY-based ECIS. First, we implement (21) and (22) by applying IMPLY and FALSE functions. The  $Sum$  output of the ECIS can be implemented by IMPLY logic as

$$[(((C_{in} \rightarrow 0) \rightarrow A_{in}) \rightarrow (((C_{in} \rightarrow (A_{in} \rightarrow 0)) \rightarrow B_{in}) \rightarrow 0))] \quad (23)$$

and its  $C_{out}$  equals  $\overline{Sum}$ .

$$C_{out_{ECIS}} = Sum_{ECIS} \rightarrow 0 \quad (24)$$

In Table 10, the serial implementation algorithm of ECIS is written in 12 steps by applying five memristors ( $A_{in}$ ,  $B_{in}$ ,  $C_{in}$ ,  $S_1$  and  $S_2$ ). In this algorithm,  $Sum$  is calculated in the tenth step, and  $C_{out}$  is calculated in the twelfth step.

Table 10: IMPLY-based implementation algorithm of ECIS.

Step	Operation	Equivalent logic
1	$S_1 = 0$	$FALSE(S_1)$
2	$S_2 = 0$	$FALSE(S_2)$
3	$A_{in} \rightarrow S_1 = S'_1$	$NOT(A_{in})$
4	$C_{in} \rightarrow S_2 = S'_2$	$NOT(C_{in})$
5	$S'_2 \rightarrow A_{in} = A'_{in}$	$NOT(C_{in}) \rightarrow A_{in}$
6	$C_{in} \rightarrow S'_1 = S''_1$	$C_{in} \rightarrow NOT(A_{in})$
7	$S''_1 \rightarrow B_{in} = B'_{in}$	$(C_{in} \rightarrow NOT(A_{in})) \rightarrow B_{in}$
8	$C_{in} = 0$	$FALSE(C_{in})$
9	$B'_{in} \rightarrow C_{in} = C'_{in}$	$NOT((C_{in} \rightarrow NOT(A_{in})) \rightarrow B_{in})$
10	$A'_{in} \rightarrow C'_{in} = C''_{in}$	$Sum = [(((C_{in} \rightarrow 0) \rightarrow A_{in}) \rightarrow (((C_{in} \rightarrow (A_{in} \rightarrow 0)) \rightarrow B_{in}) \rightarrow 0))]$
11	$B_{in} = 0$	$FALSE(B_{in})$
12	$C''_{in} \rightarrow B_{in} = B'_{in}$	$C_{out} = \overline{Sum}$

### 3.3 Summary of the proposed approximate full adders

This subsection summarizes the properties of the proposed approximate full adders introduced in subsections 3.1 and 3.2. The main features of ICIS1-3 and ECIS, including error analysis metrics, number of computational steps, and required number of memristors, are written in Table 11.

Table 11: The circuit and error evaluation criteria of ICIS1-3 and ECIS.

Approximate full adder	No. of steps	No. of memristors	ED	MED	NMED
ICIS1	6	4	3	0.375	0.125
ICIS2	6	4	3	0.375	0.125
ICIS3	6	4	3	0.375	0.125
ECIS	12	5	2	0.25	0.0833

## 4 Simulation results and comparison

In this section, the proposed approximate full adders and SOA [3,20,31,37] are compared with each other by circuit evaluation criteria (subsection 4.1), error analysis metrics (subsection 4.2), and image quality metrics (subsection 4.3). Then, in subsection 4.4, the results of these three simulations are compared with each other by a *FOM*.

Table 12: Setup values of VTEAM model and IMPLY logic [3, 10, 31].

Parameter	Value	Parameter	Value	Parameter	Value
$v_{off}$	0.7 V	$v_{on}$	-10 mV	$\alpha_{off}$	3
$\alpha_{on}$	3	$R_{off}$	1 M $\Omega$	$R_{on}$	10 k $\Omega$
$k_{on}$	-0.5 $\frac{nm}{s}$	$k_{off}$	1 $\frac{cm}{s}$	$w_{off}$	0 nm
$w_{on}$	3 nm	$w_C$	107 pm	$a_{off}$	3 nm
$a_{on}$	0 nm	$v_{set}$	1 V	$v_{reset}$	1 V
$v_{cond}$	900 mV	$R_G$	40 K $\Omega$	$t_{pulse}$	30 $\mu s$

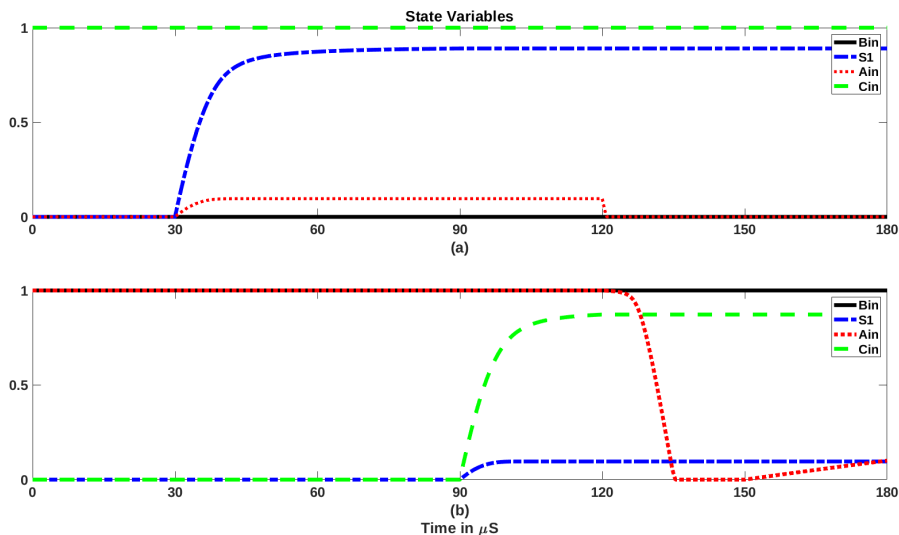
#### 4.1 Circuit-level simulation and analysis

The hardware complexity of the proposed circuits is reduced by applying approximate computing. Approximate full adders' circuit-level simulation results (energy consumption, computational steps, and estimation of area dissipation) compared to the exact [20, 37] and approximate full adders [3, 31] are critical in determining the improvement of circuit evaluation criteria. Accordingly, it is possible to calculate the improvement of circuit evaluation criteria and apply the simulation results to analyze the application of the proposed circuits in larger computing structures. LTSPICE simulator and Voltage ThrEshold Adaptive Memristor (VTEAM) model are applied for circuit-level simulation of the proposed circuits and SOA [3, 20, 31, 37]. The semi-serial architecture's compatibility with the crossbar array is moderate [41]; hence, the proposed circuits designed based on serial architecture are not comparable with the semi-serial AFA [32]. In Table 12, the parameters of the applied memristor model and the required parameters for simulating the IMPLY function are written.

The proposed circuits are simulated by applying the parameters reported in Table 12 and all the input patterns considered. According to the simulation results, the proposed algorithms for implementing ICIS1-3 and ECIS led to correct results in all cases. Two output waveforms of each of the circuits, including inputs that lead to approximate and exact outputs, as showcased, are shown in Figures 6-9. In Figures 6-9, logic '1' corresponds to LRS, and logic '0' corresponds to HRS.

ICIS1-3 calculate the  $Sum$  and  $C_{out}$  outputs in 6 computational steps. Each computational step is considered 30  $\mu s$ . The  $C_{out}$  and  $Sum$  outputs of each ICIS1-3 are computed in the fourth (90-120  $\mu s$ ) and sixth (150-180  $\mu s$ ) computational steps. Figures 6-8 show the output waveforms of the ICIS1-3. In each of Figures 6-8, two different inputs and corresponding outputs of each input can be seen.

The output waveforms of the ECIS for two input states can be seen in Figure 9. The inputs of  $A_{in}B_{in}C_{in}="000"$  and  $A_{in}B_{in}C_{in}="101"$  applied to ECIS, its implementation algorithm ran, and the output waveforms depicted in Figure 9. In this circuit,  $Sum$  is stored in memristor ' $C_{in}$ ' in the tenth step (270-300  $\mu s$ ), and  $C_{out}$  is stored in memristor ' $B_{in}$ ' in the twelfth step (330-360  $\mu s$ ).


 Figure 6: ICIS1's waveforms: (a)  $A_{in}B_{in}C_{in}="001"$ , and (b)  $A_{in}B_{in}C_{in}="110"$ .

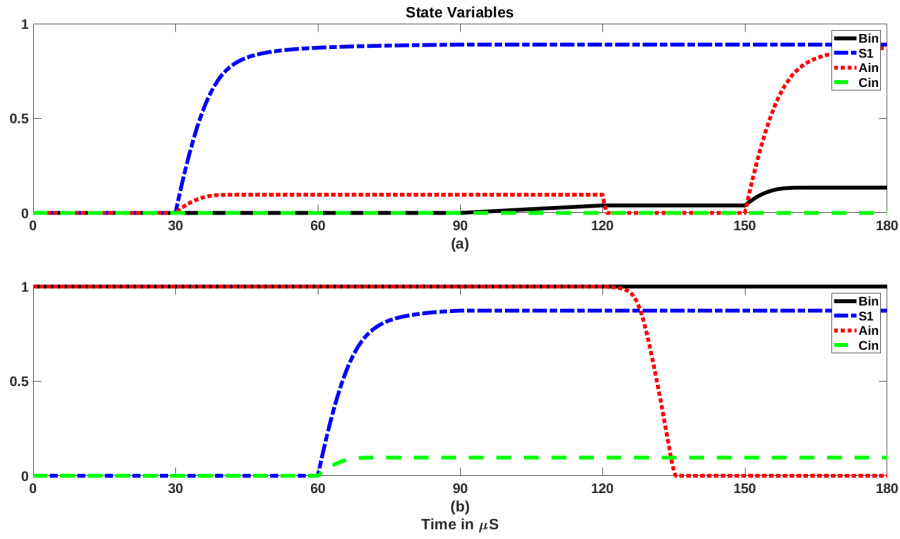


Figure 7: ICIS2's waveforms: (a)  $A_{in}B_{in}C_{in}="000"$ , and (b)  $A_{in}B_{in}C_{in}="110"$ .

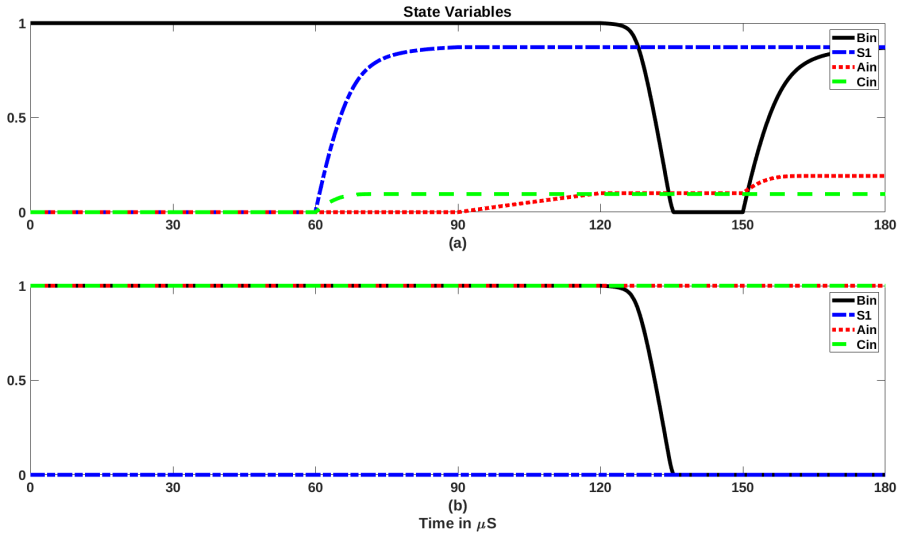


Figure 8: ICIS3's waveforms: (a)  $A_{in}B_{in}C_{in}="010"$ , and (b)  $A_{in}B_{in}C_{in}="111"$ .

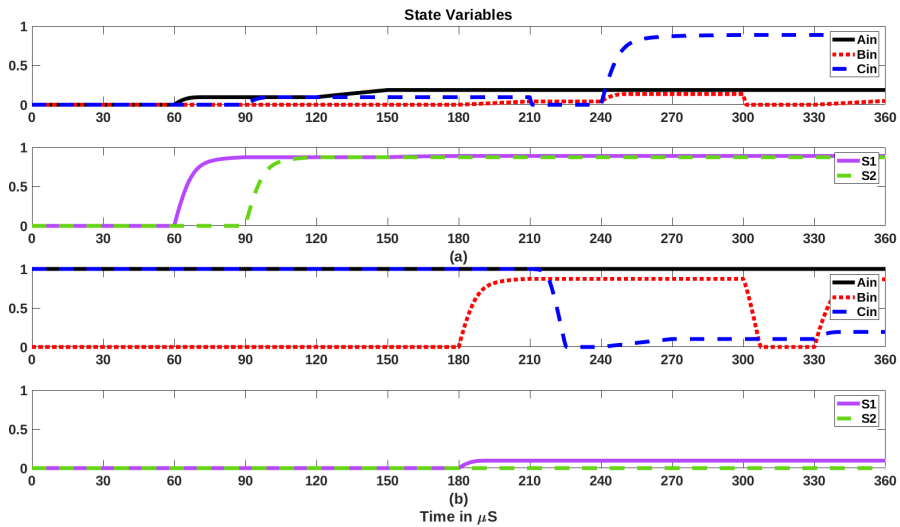


Figure 9: ECIS's waveforms: (a)  $A_{in}B_{in}C_{in}="000"$ , and (b)  $A_{in}B_{in}C_{in}="101"$ .

Approximate full adders can be applied in n-bit approximate adders in different ways. Generally, approximate full adders are placed in the LSBs, and the exact full adders are applied in the MSBs to control the accuracy of computations. An approximate 8-bit Ripple Carry Adder (RCA) structure is shown in Figure 10. In this structure, 5 LSBs are computed by approximate full adders, and exact full adders calculate 3 MSBs. Three scenarios are considered to report and compare the results of different simulations in this article. The structure in which the mentioned scenarios are examined is the 8-bit approximate RCA. Three, four, and five LSBs of the 8-bit RCA structure are calculated by the approximate full adders in the first, second, and third scenarios, respectively. In the approximate RCA structures of scenarios 1-3, the MSBs (5, 4, and 3, respectively) are calculated by the exact full adders.

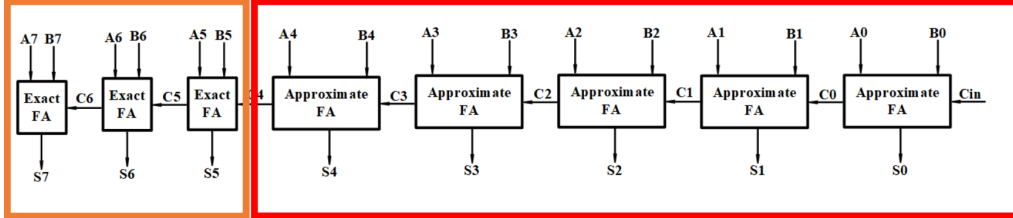


Figure 10: The third scenario's RCA structure [4].

Table 13: Comparison of the number of computational steps and memristors of ICIS1-3, ECIS, SIAFA1-4 [3], SAFAN [31], and exact full adders in [20] and [37].

Serial full adder (exact and approximate)	No. of steps		No. of memristors	
	n	n=8-bit	n	n=8-bit
Exact 1 [20]	22n	176	2n+3	19
Exact 2 [37]	23n	184	2n+3	19
Scenario 1: five most significant full adders are exact.				
SIAFA1 [3]	$8(n-5)+22(n-3)$	134	2n+3	19
SIAFA2 [3]	$10(n-5)+22(n-3)$	140	2n+3	19
SIAFA3 [3]	$8(n-5)+22(n-3)$	134	2n+3	19
SIAFA4 [3]	$8(n-5)+22(n-3)$	134	2n+3	19
SAFAN [31]	$7(n-5)+22(n-3)$	131	2n+3	19
ICIS1	$6(n-5)+22(n-3)$	128	2n+3	19
ICIS2	$6(n-5)+22(n-3)$	128	2n+3	19
ICIS3	$6(n-5)+22(n-3)$	128	2n+3	19
ECIS	$12(n-5)+22(n-3)$	146	2n+3	19
Scenario 2: four most significant full adders are exact.				
SIAFA1 [3]	$8(n-4)+22(n-4)$	120	2n+3	19
SIAFA2 [3]	$10(n-4)+22(n-4)$	128	2n+3	19
SIAFA3 [3]	$8(n-4)+22(n-4)$	120	2n+3	19
SIAFA4 [3]	$8(n-4)+22(n-4)$	120	2n+3	19
SAFAN [31]	$7(n-4)+22(n-4)$	116	2n+3	19
ICIS1	$6(n-4)+22(n-4)$	112	2n+3	19
ICIS2	$6(n-4)+22(n-4)$	112	2n+3	19
ICIS3	$6(n-4)+22(n-4)$	112	2n+3	19
ECIS	$12(n-4)+22(n-4)$	136	2n+3	19
Scenario 3: three most significant full adders are exact.				
SIAFA1 [3]	$8(n-3)+22(n-5)$	106	2n+3	19
SIAFA2 [3]	$10(n-3)+22(n-5)$	116	2n+3	19
SIAFA3 [3]	$8(n-3)+22(n-5)$	106	2n+3	19
SIAFA4 [3]	$8(n-3)+22(n-5)$	106	2n+3	19
SAFAN [31]	$7(n-3)+22(n-5)$	101	2n+3	19
ICIS1	$6(n-3)+22(n-5)$	96	2n+3	19
ICIS2	$6(n-3)+22(n-5)$	96	2n+3	19
ICIS3	$6(n-3)+22(n-5)$	96	2n+3	19
ECIS	$12(n-3)+22(n-5)$	126	2n+3	19

In Table 13, the proposed approximate full adders are compared with the approximate and exact full adders proposed in [3, 20, 31, 37] by different circuit evaluation criteria. According to the results of Table 13, all exact and approximate n-bit adders need  $2n+3$  memristors to perform the two-operands addition. The implementation

algorithms of approximate full adders ICIS1-3, SIAFA1 [3], SIAFA3 [3], SIAFA4 [3], and SAFAN [31] need four memristors (3 input memristors and one work memristor). However, exact full adders applied in MSBs of n-bit approximate RCA structures need two work memristors. So, there is a need for 2n input memristors, a memristor for the  $C_{in}$ , and two work memristors. Due to this fact, applying the approximate full adders in the LSBs of n-bit approximate RCA structures does not improve the area factor.

The number of computational steps required to calculate the final results of the exact and approximate n-bit adder structures applying the proposed approximate full adders is reported in Table 13. In n-bit approximate RCA structures,  $m_1$  LSBs are calculated by applying the approximate full adders, and  $m_2$  MSBs ( $m_2 = n - m_1$ ) are computed applying the exact full adders. The full adder proposed in [20] is applied in the MSBs. So the total number of computational steps of an n-bit approximate RCA adder can be calculated by (25). In (25),  $\alpha$  refers to the number of computational steps of the desired approximate full adder, e.g.,  $\alpha$  is 6 for ICIS1 and 12 for ECIS.

$$Total\ No.\ of\ steps = \alpha(n - m_2) + 22(n - m_1) \tag{25}$$

The number of computational steps improved by 2%-17% compared to the SIAFA1-4 [3] and SAFAN [31] and 27%-48% compared to 8-bit exact adders by applying ICIS1-3 in scenarios 1-3 (See (25)). The number of computational steps increases 4%-24% when the ECIS is applied in the structures of scenarios 1-3 instead of ICIS1-3, SIAFA1-4 [3], and SAFAN [31]. However, two things should be noted: (1) the accuracy of computations of ECIS is higher than ICIS1-3, SIAFA1-4 [3], and SAFAN [31], and (2) the number of computational steps when ECIS is placed in the 8-bit adders of scenarios 1-3 is reduced 17%-32% compared to the 8-bit exact adders [20,37].

Energy consumption is one of the most critical circuit analysis metrics. One of the main goals of applying approximate computing in the design of arithmetic circuits is to reduce energy consumption. The LTSPICE energy calculation tool is applied to calculate the energy consumption of the proposed approximate full adders and SOA [3,20,31,37]. First, the sum of the energy consumption of the memristors involved in the computations is measured for each input state of the full adder cell [3]. The average energy consumption of all the input states of the full adder cell is reported as the energy consumption estimation of the full adder cell in Table 14 [3]. According to the results of Table 14, ICIS1-3 have almost equal energy consumption. Based on their implementation algorithms, these three circuits require four memristors to compute their outputs in six computational steps. Their energy consumption is almost equal because of the same number of computational steps and required memristors. The energy consumption of each exact or approximate full adder can be compared with other full adders based on the number of computational steps and the number of memristors required.

Table 14: Approximate and exact full adders energy consumption comparison.

Serial full adder (exact and approximate)	Energy Consumption ( $\times 10^{-9}J$ )	Improvement percentage over [37]
Exact 1 [20]	1.90859	5 %
Exact 2 [37]	2.00727	-
SIAFA1 [3]	0.67221	67 %
SIAFA2 [3]	0.86032	57 %
SIAFA3 [3]	0.67221	67 %
SIAFA4 [3]	0.67086	67 %
SAFAN [31]	0.64282	68 %
ICIS1	0.50709	75 %
ICIS2	0.50705	75 %
ICIS3	0.50705	75 %
ECIS	1.02631	49 %

According to the results reported in Table 14, the order of energy consumption between the proposed approximate full adders and SOA [3,31] is as follows: ICIS2 and ICIS3, ICIS1, SAFAN [31], SIAFA4 [3], SIAFA1 [3], SIAFA3 [3], SIAFA2 [3], and ECIS.

The energy consumption improvement of the proposed approximate full adders compared to the exact full adder [37] is written in Table 14. ICIS1-3 improved the energy consumption by 20%-75% compared to the

SOA [3, 20, 31, 37]. The energy consumption of the ECIS is higher than the other approximate full adders (ICIS 1-3, SAFAN [31], and SIAFA1-4 [3]). However, this approximate full adder increases computations' accuracy compared to the others. The ECIS improved the energy consumption of exact full adders [20, 37] by 46% and 49%.

In general, the energy consumption of n-bit approximate adders applying  $m_1$  exact full adders [20] in MSBs and  $m_2$  approximate ones in LSBs of RCA structure can be estimated by (26).  $\beta$  is equal to the energy consumption of each approximate full adder.

$$\text{Total energy dissipation} = \beta(n - m_1)nJ + 1.90859(n - m_2)nJ \quad (26)$$

## 4.2 Error analysis simulation and comparison

Two items should always be evaluated and analyzed in approximate computing. The first item, the circuit analysis metrics improvement, is analyzed in the last subsection. The computation's accuracy, as the second main item in approximate computing, is analyzed in this subsection. Estimating the error magnitude of an error-tolerant application's outputs is possible by examining error analysis metrics [42]. Error analysis metrics such as MED and NMED can be applied to analyze the proposed circuits' accuracy. The smaller the error analysis metrics, the higher the computations' accuracy. All possible input combinations (65536 different input patterns) are applied to the 8-bit approximate adders of scenarios 1-3 designed based on ICIS1-3, ECIS, SIAFA1-4 [3], and SAFAN [31] to calculate the error analysis metrics. The results of error analysis metrics are shown in Table 15.

Table 15: Simulation results of error-analysis metrics.

Approximate full adder	MED	NMED
Scenario 1: five most significant full adders are exact.		
SIAFA1 [3]	2.062	0.004
SIAFA2 [3]	2.656	0.0052
SIAFA3 [3]	2.062	0.004
SIAFA4 [3]	2.625	0.0051
SAFAN [31]	2.9375	0.0057
ICIS1	2.156	0.0042
ICIS2	2.25	0.0044
ICIS3	2.25	0.0044
ECIS	1.718	0.0033
Scenario 2: four most significant full adders are exact.		
SIAFA1 [3]	4.351	0.0085
SIAFA2 [3]	6.1718	0.0121
SIAFA3 [3]	4.351	0.0085
SIAFA4 [3]	5.3125	0.0104
SAFAN [31]	5.78125	0.0113
ICIS1	4.7265	0.0092
ICIS2	4.4687	0.0087
ICIS3	4.4687	0.0087
ECIS	3.6171	0.007
Scenario 3: three most significant full adders are exact.		
SIAFA1 [3]	8.8554	0.0173
SIAFA2 [3]	13.498	0.0264
SIAFA3 [3]	8.8554	0.0173
SIAFA4 [3]	10.6562	0.0208
SAFAN [31]	11.04687	0.02166
ICIS1	9.8886	0.0193
ICIS2	8.9121	0.0174
ICIS3	8.9121	0.0174
ECIS	7.3769	0.0144

The main goal of proposing the ECIS and overcoming its hardware complexity compared to the ICIS1-3 is to prevent the spread of inexact  $C_{out}$  from LSBs to the MSBs and increase the accuracy of computations. Error



analysis metrics (e.g., MED and NMED) are minimum when the ECIS is applied in the structure of scenarios 1-3, according to the results of Table 15. The accuracy of computations increases when the ECIS full adder is applied in larger arithmetic structures compared to the ICIS1-3, SIAFA1-4 [3], and SAFAN [31] based on the results of Table 15. So, the primary purpose of proposing the ECIS is achieved. The error analysis metrics of ICIS2 and ICIS3 full adders are equal, based on their truth tables, in scenarios 1-3, and the results are reported in Table 15. The ED of these two approximate full adders equals 3, and their computations' accuracy is lower than ECIS (ED=2). The computations' accuracy decreased by 9%, 2%, and 1%, respectively, by applying the ICIS2 and ICIS3 instead of SIAFA1 [3] and SIAFA3 [3] in the structures of scenarios 1-3. It should be mentioned that the number of computational cycles has also decreased by 5%, 7%, and 9% by applying the ICIS2 and ICIS3 instead of SIAFA1 [3] and SIAFA3 [3] in these three scenarios, respectively. The computations' accuracy of ICIS1 is lower than the other proposed approximate full adders in this article, SIAFA1 [3], and SIAFA3 [3] in scenarios 1-3. The accuracy of computations decreased from 4%-10% by applying ICIS1 instead of SIAFA1 [3] and SIAFA3 [3] in scenarios 1-3, but the computational steps improved by 5%-9% in these scenarios. This approximate full adder increases the accuracy of computations in scenarios 1-3 compared to SIAFA2 [3], SIAFA4 [3], and SAFAN [31].

### 4.3 Application-level simulation and comparison

The reduction of circuit complexity in approximate computing should be accompanied by acceptable accuracy reduction so that this computational method can be effectively applied in error-resilient applications. Image processing as an error-resilient application is a complex and data-intensive application widely applied in daily human lives [3]. This application is a suitable candidate for in-memory approximate computing by applying memristors [3,9]. So, the proposed approximate full adders are applied in the computational structures of scenarios 1-3 and are simulated behaviorally in three different image processing applications of image addition, motion detection, and grayscale filter. PSNR, SSIM, and MSSIM are applied to evaluate the output image quality metrics. The proposed full adders have equal single-bit error analysis metrics but do not have equal output image quality metrics in image processing applications. The reason is that the input distributions in images differ from those in the error analysis simulations [3].

#### 4.3.1 Image addition application

Improving the quality of the images and masking them are the applications of image addition [3]. Image addition is a fundamental and widely used application in image processing. In the image addition application, the pixels  $P_{1,ij}$  and  $P_{2,ij}$  of the two input images are added together, and the result is stored in the output pixel  $P_{O,ij}$ .

The behavioral simulation results of ECIS and ICIS1-3 that are applied in the image addition application in the computational structures of scenarios 1-3 are tabulated in Table 16. The third scenario's output images for the proposed approximate full adders (ICIS1-3 and ECIS) are illustrated in Figure 11.

According to Table 16, the highest quality of the output images is obtained when ECIS is applied in the computational structures of scenarios 1-3 introduced in subsection 4.1. The lowest quality of the output images (PSNR) corresponded to SIAFA2 [3] and SAFAN [31]. Also, the quality of output images is acceptable when ICIS1-3 are applied in the computational structures of scenarios 1-3 (PSNR is higher than 30 dB). The output image quality is higher than 45 dB when the ECIS is applied in scenario 1. The quality of the output images varied between 43.94 dB and 44.5 dB when ICIS1-3, SIAFA1 [3], and SIAFA3 [3] are applied in the computational structure of scenario 1. The quality of the output images is higher than 39 dB only when ECIS is applied in the second scenario's computing structure. The quality of the output images is between 38-39 dB when ICIS1-3, SIAFA1 [3], and SIAFA3 [3] are applied in the second scenario's RCA structure. The outputs of the image addition application have the least image quality when SAFAN [31] and SIAFA2 [3] are applied in the second scenario's arithmetic architecture (PSNR is less than 38 dB). The quality of output images is higher than other circuits by applying ECIS and ICIS3 in the third scenario (PSNR is higher than 33 dB). The outputs are acceptable (PSNR is higher than 30 dB) when ICIS1, ICIS2, SIAFA1 [3], SIAFA3 [3], SIAFA4 [3], and SAFAN [31] are applied in the LSBs of the third scenario's approximate adder. Suppose the number of approximate full adders (ECIS, ICIS1-3, SIAFA1-4 [3], and SAFAN [31]) increases in the LSBs of an 8-bit RCA to six bits. In that case, the image quality of the outputs generated by these RCAs is less than 30 dB, and the output images are unacceptable.

Table 16: Image quality metrics of image addition application.

Approximate full adder	PSNR (dB)	SSIM	MSSIM
Scenario 1: five most significant full adders are exact.			
SIAFA1 [3]	44.5148	0.9899	0.99
SIAFA2 [3]	41.9674	0.9858	0.9861
SIAFA3 [3]	44.5222	0.9898	0.99
SIAFA4 [3]	43.7483	0.9878	0.988
SAFAN [31]	41.8917	0.994	0.994
ICIS1	44.1644	0.9909	0.991
ICIS2	43.9423	0.9888	0.9889
ICIS3	43.9769	0.9886	0.9887
ECIS	45.1444	0.9918	0.9919
Scenario 2: four most significant full adders are exact.			
SIAFA1 [3]	38.67	0.9644	0.9649
SIAFA2 [3]	35.4576	0.9425	0.9436
SIAFA3 [3]	38.8399	0.9638	0.9644
SIAFA4 [3]	37.8083	0.959	0.9597
SAFAN [31]	36.6395	0.9793	0.9796
ICIS1	38.2287	0.9654	0.966
ICIS2	38.545	0.9632	0.9636
ICIS3	38.4096	0.961	0.9615
ECIS	39.4711	0.9702	0.9706
Scenario 3: three most significant full adders are exact.			
SIAFA1 [3]	32.9823	0.8974	0.8996
SIAFA2 [3]	28.2504	0.8156	0.8166
SIAFA3 [3]	32.6497	0.8905	0.8915
SIAFA4 [3]	32.0442	0.8931	0.8956
SAFAN [31]	30.5866	0.9297	0.9298
ICIS1	32.0474	0.9006	0.9027
ICIS2	32.9714	0.896	0.8978
ICIS3	33.0242	0.8927	0.8956
ECIS	33.7765	0.9128	0.9143

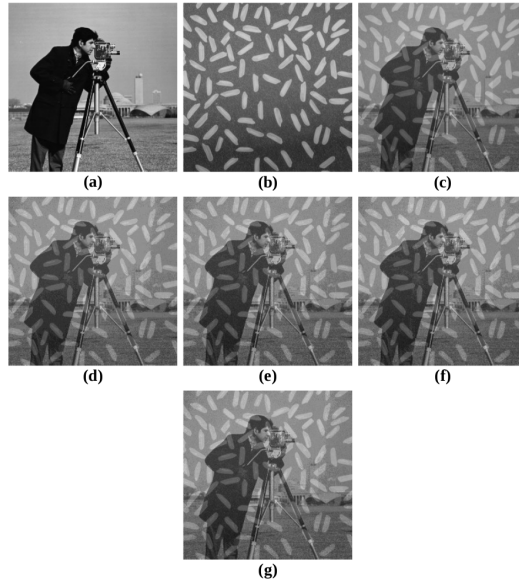


Figure 11: The image addition simulation outputs based on the third scenario's RCA structure: (a) cameraman, (b) rice, (c) exact output, (d) ICIS1, (e) ICIS2, (f) ICIS3, and (g) ECIS.

### 4.3.2 Motion Detection Application

Subtraction of two images is applied to detect motion in images [3]. The corresponding pixels of two images are subtracted from each other, and the result is stored as an output image. In this article, the 2's complement addition method is applied in the approximate adders of scenarios 1-3 to perform subtraction.

Two consecutive frames are placed in the subfigures 12a and 12b. The result of the subtraction of these two

consecutive frames applying an exact 8-bit adder is shown in the subfigure 12c. Subfigures 12d-12g are the output images obtained from the subtraction of these two consecutive frames applying the proposed approximate full adders in the RCA of scenario 2. The image quality metrics of the output images in different scenarios are written in Table 17.

Table 17: Image quality metrics of motion detection application.

Approximate full adder	PSNR (dB)	SSIM	MSSIM
Scenario 1: five most significant full adders are exact.			
SIAFA1 [3]	41.5919	0.7711	0.7901
SIAFA2 [3]	43.5407	0.9678	0.9874
SIAFA3 [3]	41.8705	0.7905	0.8103
SIAFA4 [3]	45.5121	0.9534	0.9693
SAFAN [31]	49.7504	0.9863	0.9905
ICIS1	45.564	0.9703	0.9886
ICIS2	45.8315	0.9685	0.9863
ICIS3	45.8356	0.9682	0.9861
ECIS	46.1802	0.9661	0.9811
Scenario 2: four most significant full adders are exact.			
SIAFA1 [3]	37.4131	0.6405	0.6705
SIAFA2 [3]	37.5605	0.9338	0.9652
SIAFA3 [3]	36.8613	0.5993	0.6302
SIAFA4 [3]	40.3861	0.9131	0.9423
SAFAN [31]	44.0205	0.9798	0.9857
ICIS1	40.3774	0.9409	0.9713
ICIS2	40.5783	0.9351	0.968
ICIS3	40.715	0.9349	0.9685
ECIS	40.7888	0.9303	0.9588
Scenario 3: three most significant full adders are exact.			
SIAFA1 [3]	32.6121	0.508	0.5404
SIAFA2 [3]	31.6441	0.8991	0.9265
SIAFA3 [3]	32.4096	0.4747	0.5094
SIAFA4 [3]	35.0436	0.8664	0.902
SAFAN [31]	37.5336	0.9667	0.9727
ICIS1	34.928	0.9104	0.9421
ICIS2	35.2479	0.8956	0.9363
ICIS3	35.3686	0.8959	0.937
ECIS	35.3095	0.8873	0.9226

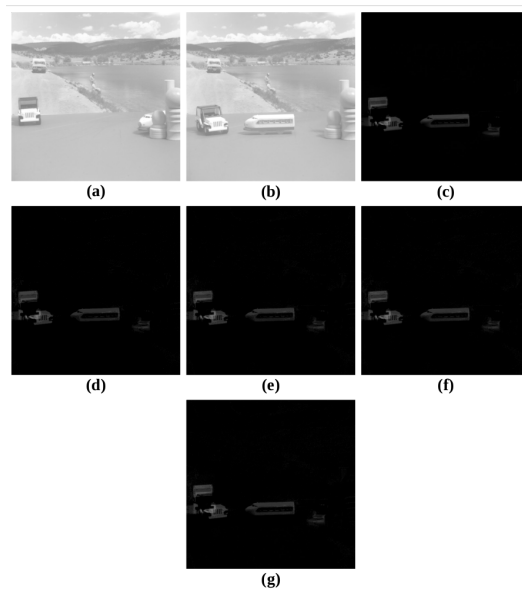


Figure 12: The motion detection simulation outputs based on the second scenario's RCA structure: (a) first image [43], (b) second image [43], (c) exact output, (d) ICIS1, (e) ICIS2, (f) ICIS3, and (g) ECIS.

According to the results of Table 17, ECIS and ICIS1-3 are among the first six approximate full adders in the application of motion detection in all three scenarios. When the proposed circuits are applied in the computational structures of scenarios 1-3, the quality of the output images is higher than 45 dB, 40 dB, and 34.9 dB, respectively. The image quality metrics of the outputs of motion detection application are not acceptable if the number of approximate full adders in the LSBs of an 8-bit approximate adder structure is changed from 5 to 6 (only the two MSBs are computed applying the exact full adder). The PSNR of output images is higher than 29,5 dB, but the motions could not be detected by applying all four proposed approximate full adders in this structure. The same results are obtained by applying the SOA [3,31] in this RCA, and it is impossible to detect motion by applying these approximate full adders.

### 4.3.3 Grayscale filter

Red, Green, and Blue (RGB) images are made of an  $m \times n \times 3$  vector where  $m \times n$  defines the image's dimensions. Each RGB image consists of three layers R, G, and B. Combining these three layers in different ways creates an RGB image. In this paper, like [3,31], each pixel's R, G, and B values are added together to convert RGB images to grayscale by the RCAs of scenarios 1-3 designed based on ECIS, ICIS1-3, SIAFA1-4 [3], and SAFAN [31]. Then the sum of these values is divided by three and stored as the output grayscale pixel. It should be noted that the division is computed accurately [3].

The simulation results of this image processing application applying the proposed approximate full adders in the computational structures of scenarios 1-3 are written in Table 18. Figure 13 shows the grayscale output images computed by the approximate RCAs of scenario three made by the proposed circuits.

Table 18: Image quality metrics of grayscale filter.

Approximate full adder	PSNR (dB)	SSIM	MSSIM
Scenario 1: five most significant full adders are exact.			
SIAFA1 [3]	47.1982	0.9911	0.999
SIAFA2 [3]	43.1339	0.9833	0.9977
SIAFA3 [3]	47.2496	0.9914	0.999
SIAFA4 [3]	43.0565	0.9841	0.997
SAFAN [31]	42.2449	0.9905	0.9974
ICIS1	44.7574	0.9878	0.9984
ICIS2	45.4874	0.9911	0.9987
ICIS3	44.9761	0.9903	0.9986
ECIS	47.5379	0.9925	0.9991
Scenario 2: four most significant full adders are exact.			
SIAFA1 [3]	41.4201	0.9693	0.9957
SIAFA2 [3]	35.9998	0.9263	0.9874
SIAFA3 [3]	41.2315	0.9684	0.9956
SIAFA4 [3]	36.9634	0.9451	0.989
SAFAN [31]	36.0101	0.9625	0.9886
ICIS1	37.9719	0.9474	0.9911
ICIS2	40.1764	0.9693	0.9953
ICIS3	39.9446	0.9679	0.9952
ECIS	41.9064	0.973	0.9966
Scenario 3: three most significant full adders are exact.			
SIAFA1 [3]	35.5671	0.9019	0.9778
SIAFA2 [3]	28.4883	0.7576	0.9317
SIAFA3 [3]	35.3588	0.8916	0.9794
SIAFA4 [3]	31.5146	0.8525	0.9589
SAFAN [31]	28.9472	0.8633	0.9482
ICIS1	30.3889	0.8163	0.9441
ICIS2	33.9817	0.9011	0.973
ICIS3	34.4268	0.8992	0.9782
ECIS	35.8643	0.9094	0.9814

The output images have the best image quality metrics when ECIS is applied in scenarios 1-3. The output images of other proposed approximate full adders (ICIS1-3) are also acceptable in scenarios 1-3. In the first, second, and third scenarios, the PSNR of the output images generated by the proposed approximate full adders is higher than 44.7 dB, 37.9 dB, and 30 dB, respectively.

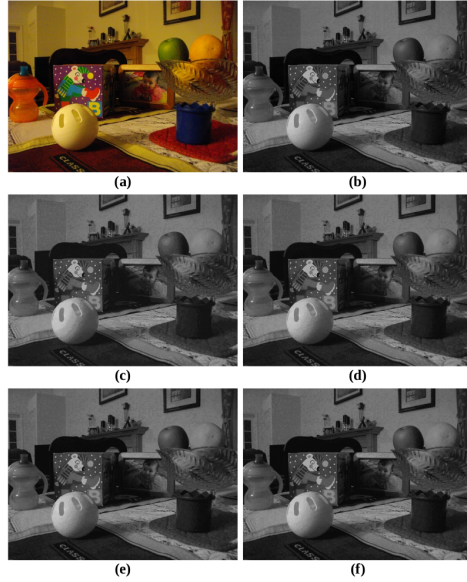


Figure 13: The grayscale filter simulation outputs based on the third scenario’s RCA structure: (a) RGB image, (b) exact output, (c) ICIS1, (d) ICIS2, (e) ICIS3, and (f) ECIS.

The simulation result of this application is also of good quality, even though a small shadow is formed on the output image if the ECIS is applied in the six LSBs of an 8-bit approximate RCA (two MSBs are exact). The PSNR of the output image in this scenario is 29.8814 dB. The output’s image quality metrics are unacceptable when the ICIS1 is applied in the six LSBs of an 8-bit approximate RCA (PSNR is 23.4527 dB). The output images and the grayscale filter’s performance are unacceptable (PSNR is about 27 dB) when ICIS2 and ICIS3 are also applied in the mentioned structure.

#### 4.4 Analysis of the trade-off between Circuit and Error evaluation metrics

The proposed circuits were analyzed only by circuit analysis metrics in subsection 4.1. Different error analysis criteria and image quality metrics were applied to analyze the proposed circuits in subsections 4.2, and 4.3. The reduction of accuracy in computations leads to the reduction of circuit complexity in approximate computing. We compared the proposed circuits by simultaneously considering the circuit and error evaluation criteria in this subsection. The *FOM* introduced in this article considers the Energy consumption and computational Delay Product (EDP) as circuit analysis metrics and the accuracy-related metrics of 1-NMED and PSNR according to the third scenario’s results.

This *FOM* is defined as

$$FOM = \frac{EDP}{(1 - NMED) \times PSNR} \quad (27)$$

The results of *FOM* for the proposed circuits, SIAFA1-4 [3], and SAFAN [31] are written in Table 19. The average PSNR value of three 8-bit image processing applications assessed in the last subsection is considered to calculate the *FOM*. ICIS3, ICIS2, and ICIS1 made the best trade-off between the circuit complexity and the accuracy of the computations, respectively, according to Table 19. The *FOM* computed for the ECIS is higher than ICIS1-3, SAFAN [31], SIAFA1 [3], SIAFA3 [3], and SIAFA4 [3]. However, it should be emphasized that the  $ER_{C_{out}}$  of ECIS is equal to 0, and errors do not propagate from LSBs to MSBs. This full adder’s computations’ accuracy is higher than the other approximate full adders.

The applicability of ECIS is recommended over the other proposed full adders in applications where the accuracy of computations is of great importance and limited reduction of hardware complexity is acceptable.

Table 19: The *FOM* results of the SIAFA1-4 [3], SAFAN [31], and the proposed approximate full adders in the third scenario’s RCA structure.

Approximate full adder	<i>FOM</i>
SIAFA1 [3]	29.06734
SIAFA2 [3]	40.55279
SIAFA3 [3]	29.2824
SIAFA4 [3]	29.9061
SAFAN [31]	28.61973
ICIS1	24.91743
ICIS2	23.69175
ICIS3	23.54914
ECIS	39.67634

## 5 Conclusion

We tried to take a step forward to improve the power wall problem by applying approximate computing. The ICIS1-3 are proposed to improve energy consumption by applying approximate computing and redefining approximate logic from the exact logic method. The ECIS is also proposed to increase the accuracy of computations while improving the circuit analysis metrics compared to the exact full adders. The implementation algorithms of the proposed full adders are designed by applying the IMPLY method as a stateful logic to enable the implementation of these circuits for IMP in the structure of crossbar arrays. ICIS1-3 improve the energy consumption by 21%-41% over approximate SOA and 73%-75% over the exact full adders. ICIS1-3 improve the computational steps by 14%-74% compared to SOA applying the same number of memristors as previous designs. The ECIS also reduces energy consumption by a maximum of 49% and the number of computational steps by 48% compared to exact full adders. The proposed full adders are compared with SOA by error analysis metrics and image quality criteria in three scenarios and three image processing applications. The ECIS has the highest computation accuracy in all three scenarios. ICIS1-3 have acceptable error evaluation criteria in all three scenarios and image processing applications. Circuit evaluation metrics and accuracy in computations are evaluated side by side by presenting a *FOM*. ICIS3, ICIS2, and ICIS1 have the highest ranks among other approximate full adders concerning the *FOM*, respectively.

## Author Contributions

**Seyed Erfan Fatemieh:** Conceptualization, Methodology, Software, Validation, Formal Analysis, Investigation, Data Curation, Writing - Original Draft, Writing - Review & Editing, Visualization.

**Mohammad Reza Reshadinezhad:** Software, Validation, Formal Analysis, Investigation, Resources, Writing - Review & Editing, Supervision, Project Administration.

## Acknowledgements

This research did not receive any specific grant from funding agencies in the public, commercial, or not-for-profit sectors.

## Data Availability Statement

Data is contained within the article.

## Conflicts of Interest

The authors declare no conflicts of interest.

## References

- [1] H. A. D. Nguyen, J. Yu, M. A. Lebdeh, M. Taouil, S. Hamdioui, and F. Catthoor, “A classification of memory-centric computing,” *ACM Journal on Emerging Technologies in Computing Systems (JETC)*, vol. 16, no. 2, pp. 1–26, 2020.
- [2] W. Liu, F. Lombardi, and M. Shulte, “A retrospective and prospective view of approximate computing [point of view],” *Proceedings of the IEEE*, vol. 108, no. 3, pp. 394–399, 2020.
- [3] S. E. Fatemieh, M. R. Reshadinezhad, and N. TaheriNejad, “Fast and compact serial imply-based approximate full adders applied in image processing,” *IEEE Journal on Emerging and Selected Topics in Circuits and Systems*, vol. 13, no. 1, pp. 175–188, 2023.
- [4] S. E. Fatemieh, S. S. Farahani, and M. R. Reshadinezhad, “Lahaf: Low-power, area-efficient, and high-performance approximate full adder based on static cmos,” *Sustainable Computing: Informatics and Systems*, vol. 30, p. 100529, 2021.
- [5] S. Shirinabadi Farahani and M. R. Reshadinezhad, “A new twelve-transistor approximate 4: 2 compressor in cntfet technology,” *International Journal of Electronics*, vol. 106, no. 5, pp. 691–706, 2019.
- [6] A. D. Zarandi, A. Rubio, and M. R. Reshadinezhad, “A memristor-based quaternary memory with adaptive noise tolerance,” in *2020 XXXV Conference on Design of Circuits and Integrated Systems (DCIS)*, pp. 1–6, IEEE, 2020.
- [7] N. Charmchi and M. R. Reshadinezhad, “Energy efficient design of four-operand multiplier architecture using cntfet technology,” *JOURNAL OF NANO AND ELECTRONIC PHYSICS*, vol. 10, no. 2, p. 02022, 2018.
- [8] S. S. Farahani, M. R. Reshadinezhad, and S. E. Fatemieh, “New design for error-resilient approximate multipliers used in image processing in cntfet technology,” *The Journal of Supercomputing*, vol. 80, no. 3, pp. 3694–3712, 2024.
- [9] J. Zhou, X. Yang, J. Wu, X. Zhu, X. Fang, and D. Huang, “A memristor-based architecture combining memory and image processing,” *Science China Information Sciences*, vol. 57, pp. 1–12, 2014.
- [10] D. Radakovits, N. TaheriNejad, M. Cai, T. Delaroche, and S. Mirabbasi, “A memristive multiplier using semi-serial imply-based adder,” *IEEE Transactions on Circuits and Systems I: Regular Papers*, vol. 67, no. 5, pp. 1495–1506, 2020.
- [11] S. Kvatinsky, *Memristor-based circuits and architectures*. PhD thesis, Technion-Israel Institute of Technology, Faculty of Electrical Engineering, 2014.
- [12] F. Karimi, R. Faghieh Mirzaee, A. Fakeri-Tabrizi, and A. Roohi, “Design and evaluation of ultra-fast 8-bit approximate multipliers using novel multicolumn inexact compressors,” *International Journal of Circuit Theory and Applications*, vol. n/a, no. n/a, 2023.
- [13] W. Liu, T. Zhang, E. McLarnon, M. O’Neill, P. Montuschi, and F. Lombardi, “Design and analysis of majority logic-based approximate adders and multipliers,” *IEEE transactions on emerging topics in computing*, vol. 9, no. 3, pp. 1609–1624, 2019.
- [14] S. E. Fatemieh, M. R. Reshadinezhad, and N. TaheriNejad, “Approximate in-memory computing using memristive imply logic and its application to image processing,” in *2022 IEEE International Symposium on Circuits and Systems (ISCAS)*, IEEE, 2022.
- [15] H. Jiang, C. Liu, L. Liu, F. Lombardi, and J. Han, “A review, classification, and comparative evaluation of approximate arithmetic circuits,” *ACM Journal on Emerging Technologies in Computing Systems (JETC)*, vol. 13, no. 4, pp. 1–34, 2017.
- [16] H. Jiang, F. J. H. Santiago, H. Mo, L. Liu, and J. Han, “Approximate arithmetic circuits: A survey, characterization, and recent applications,” *Proceedings of the IEEE*, vol. 108, no. 12, pp. 2108–2135, 2020.

- [17] S. Reda and M. Shafique, “Approximate circuits,” *Springer*, 2019.
- [18] V. Gupta, D. Mohapatra, A. Raghunathan, and K. Roy, “Low-power digital signal processing using approximate adders,” *IEEE Transactions on Computer-Aided Design of Integrated Circuits and Systems*, vol. 32, no. 1, pp. 124–137, 2012.
- [19] K. Alhaj Ali, *New design approaches for flexible architectures and in-memory computing based on memristor technologies*. PhD thesis, Ecole nationale supérieure Mines-Télécom Atlantique Bretagne Pays de la Loire, 2020.
- [20] S. G. Rohani and N. TaheriNejad, “An improved algorithm for imply logic based memristive full-adder,” in *2017 IEEE 30th Canadian Conference on Electrical and Computer Engineering (CCECE)*, pp. 1–4, IEEE, 2017.
- [21] S. Kvatinsky, G. Satat, N. Wald, E. G. Friedman, A. Kolodny, and U. C. Weiser, “Memristor-based material implication (imply) logic: Design principles and methodologies,” *IEEE Transactions on Very Large Scale Integration (VLSI) Systems*, vol. 22, no. 10, pp. 2054–2066, 2013.
- [22] S. G. Rohani, N. Taherinejad, and D. Radakovits, “A semiparallel full-adder in imply logic,” *IEEE Transactions on Very Large Scale Integration (VLSI) Systems*, vol. 28, no. 1, pp. 297–301, 2019.
- [23] M. Traiola, M. Barbareschi, and A. Bosio, “Estimating dynamic power consumption for memristor-based cim architecture,” *Microelectronics Reliability*, vol. 80, pp. 241–248, 2018.
- [24] N. Revanna, L. Guckert, and E. E. Swartzlander, “The future of computing arithmetic circuits implemented with memristors,” in *2017 51st Asilomar Conference on Signals, Systems, and Computers*, pp. 745–749, IEEE, 2017.
- [25] X.-Y. Wang, P.-F. Zhou, J. K. Eshraghian, C.-Y. Lin, H. H.-C. Iu, T.-C. Chang, and S.-M. Kang, “High-density memristor-cmos ternary logic family,” *IEEE Transactions on Circuits and Systems I: Regular Papers*, vol. 68, no. 1, pp. 264–274, 2020.
- [26] S. Gupta, M. Imani, and T. Rosing, “Felix: Fast and energy-efficient logic in memory,” in *2018 IEEE/ACM International Conference on Computer-Aided Design (ICCAD)*, pp. 1–7, IEEE, 2018.
- [27] I. Alouani, H. Ahangari, O. Ozturk, and S. Niar, “A novel heterogeneous approximate multiplier for low power and high performance,” *IEEE Embedded Systems Letters*, vol. 10, no. 2, pp. 45–48, 2017.
- [28] T. Zhang, W. Liu, E. McLarnon, M. O’Neill, and F. Lombardi, “Design of majority logic (ml) based approximate full adders,” in *2018 IEEE International Symposium on Circuits and Systems (ISCAS)*, pp. 1–5, IEEE, 2018.
- [29] S. E. Fatemieh and M. R. Reshadinezhad, “Power-efficient, high-psnr approximate full adder applied in error-resilient computations based on cntfets,” in *2020 20th International Symposium on Computer Architecture and Digital Systems (CADS)*, pp. 1–5, IEEE, 2020.
- [30] A. Mohammadi, M. M. Ghanatghehstani, A. S. Molahosseini, and Y. S. Mehrabani, “Image processing with high-speed and low-energy approximate arithmetic circuit,” *Sustainable Computing: Informatics and Systems*, vol. 36, p. 100785, 2022.
- [31] S. Asgari, M. R. Reshadinezhad, and S. E. Fatemieh, “Energy-efficient and fast imply-based approximate full adder applying nand gates for image processing,” *Computers and Electrical Engineering*, vol. 113, p. 109053, 2024.
- [32] F. Seiler and N. TaheriNejad, “An imply-based semi-serial approximate in-memristor adder,” in *2023 IEEE Nordic Circuits and Systems Conference (NorCAS)*, pp. 1–7, IEEE, 2023.
- [33] S. Mittal, “A survey of techniques for approximate computing,” *ACM Computing Surveys (CSUR)*, vol. 48, no. 4, pp. 1–33, 2016.



- [34] Z. Wang, A. C. Bovik, H. R. Sheikh, and E. P. Simoncelli, "Image quality assessment: from error visibility to structural similarity," *IEEE transactions on image processing*, vol. 13, no. 4, pp. 600–612, 2004.
- [35] M. Lanza, G. Molas, and I. Naveh, "The gap between academia and industry in resistive switching research," *Nature Electronics*, vol. 6, no. 4, pp. 260–263, 2023.
- [36] N. TaheriNejad, "SIXOR: Single-cycle in-memristor xor," *IEEE Transactions on Very Large Scale Integration (VLSI) Systems*, vol. 29, no. 5, pp. 925–935, 2021.
- [37] A. Karimi and A. Rezai, "Novel design for a memristor-based full adder using a new imply logic approach," *Journal of Computational Electronics*, vol. 17, no. 3, pp. 1303–1314, 2018.
- [38] S. Muthulakshmi, C. S. Dash, and S. Prabakaran, "Memristor augmented approximate adders and subtractors for image processing applications: An approach," *AEU-International Journal of Electronics and Communications*, vol. 91, pp. 91–102, 2018.
- [39] S. Muthulakshmi, C. S. Dash, and S. Prabakaran, "Memristor-based approximate adders for error resilient applications," in *Nanoelectronic Materials and Devices*, pp. 51–59, Springer, 2018.
- [40] L. Guckert and E. Swartzlander, "Optimized memristor-based ripple carry adders," in *2016 50th Asilomar Conference on Signals, Systems and Computers*, pp. 1575–1579, IEEE, 2016.
- [41] V. Lakshmi, J. Reuben, and V. Pudi, "A novel in-memory wallace tree multiplier architecture using majority logic," *IEEE Transactions on Circuits and Systems I: Regular Papers*, vol. 69, no. 3, pp. 1148–1158, 2021.
- [42] M. K. Ayub, M. A. Hanif, O. Hasan, and M. Shafique, "Peal: Probabilistic error analysis methodology for low-power approximate adders," *ACM Journal on Emerging Technologies in Computing Systems (JETC)*, vol. 17, no. 1, pp. 1–37, 2020.
- [43] University of Southern California (USC) Signal and Image Processing Institute (SIPI), *The USC-SIPI Image Database*. <https://sipi.usc.edu/database/database.php?volume=sequences>.

## Biography

**Seyed Erfan Fatemieh** was born in Isfahan, Iran, in 1996. He received his B.Sc. degree in Computer Engineering and M.Sc. degree in Computer Architecture from the University of Isfahan, Isfahan, Iran, in 2018 and 2020. He is currently a Ph.D. candidate in Computer Architecture at the University of Isfahan, Isfahan, Iran. His research interests include In-memory Computing, Digital VLSI, Computer Arithmetic, and Quantum Computing and Reversible Circuits.

**Mohammad Reza Reshadinezhad** was born in Isfahan, Iran, in 1959. He received his B.S. and M.S. degrees from the Electrical Engineering Department of the University of Wisconsin, Milwaukee, USA, in 1982 and 1985, respectively. He has been in the position of lecturer as faculty of computer engineering at the University of Isfahan since 1991. He also received a Ph.D. Degree in computer architecture from Shahid Beheshti University, Tehran, Iran, in 2012. He is currently an Associate Professor in the Faculty of Computer Engineering at the University of Isfahan. His research interests are Digital Arithmetic, Nanotechnology concerning CNTFET, VLSI Implementation, and Cryptography.